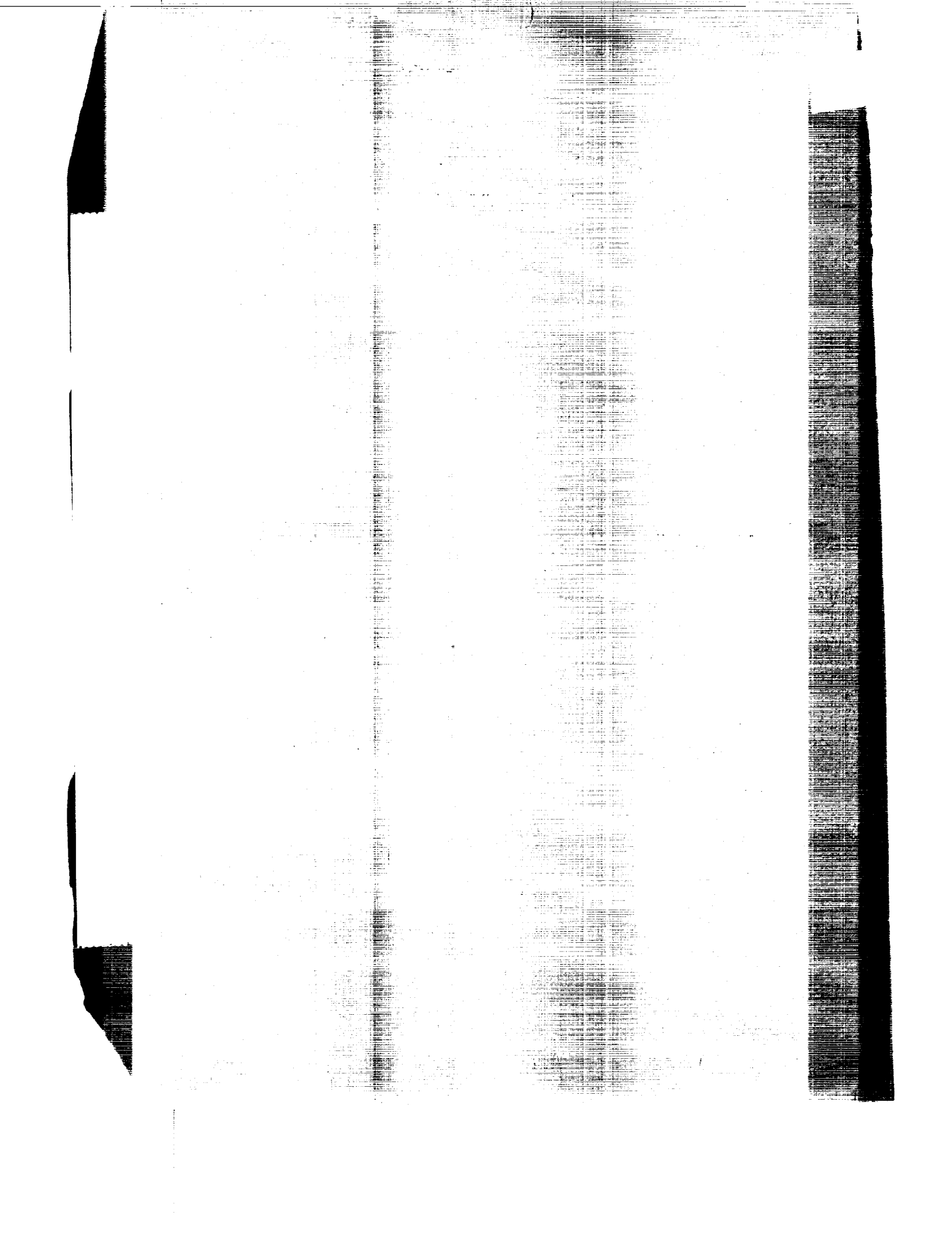


REPRODUCED BY  
**NATIONAL TECHNICAL  
INFORMATION SERVICE**  
U. S. DEPARTMENT OF COMMERCE  
SPRINGFIELD, VA. 22161



NATIONAL ADVISORY COMMITTEE FOR AERONAUTICS

TECHNICAL MEMORANDUM NO. 605

FLAT SHEET METAL GIRDERS WITH VERY THIN METAL WEB\*

By Herbert Wagner

PART II

Sheet Metal Girders with Spars Resistant to Bending -  
Oblique Uprights - Stiffness

Noting that the stiffness of the girder increases very rapidly as  $\beta$  increases, the result can be summed up as follows: When the cross stress preponderates in one direction and when the web plate is to be given the dimensions commensurate to its stresses, it is advisable (regardless of any ensuing structural difficulties) to set the uprights at about  $\beta = 120^\circ$ , thereby lowering the weight of the plate wall 15 per cent (in contrast to  $\beta = 90^\circ$ ), and raising the stiffness 55 per cent. But, when the cross stresses alternate and are approximately of the same intensity in both directions, or, if the web plate thickness is determined by other structural reasons, then  $\beta = 90^\circ$  should be chosen.

Non-parallel Spars

In this case (Fig. 14) part of the cross stress is carried by the spars regardless of whether the web plate is under ten-

\*"Ebene Blechwandträger mit sehr dünnen Stegblech." From Zeitschrift für Flugtechnik und Motorluftschiffahrt, Vol. 20, Nos. 9, 10 and 11, May 14 & 28, and June 14, 1929. For Part I, see N.A.C.A. Technical Memorandum No. 604.

sion or shear.

We begin our discussion with the simple case of a web plate subjected to shear, but assume the cross section of the spars to be large with respect to that of the web and further presume that the bending moment is solely taken up by the spars and that the cross stress  $Q_s$  taken up from the web is evenly distributed over it.

Now let us determine the web stress at cut 1, for the sheet metal girder shown in Figure 14.  $Q$  is to represent the resultant cross stress of the individual stresses  $Q_1, Q_2$ , etc., to the left of 1. We apply the inside stresses transmitted at 1 as outside stresses and bring the left portion of the girder in equilibrium. With  $X_0$  and  $X_u$  as the  $x$ -components of the spar stresses, we have

$$X_0 = (-X_u), \quad \text{for } x \text{ components,}$$

$$X \tan \theta_0 + X \tan \theta_u + Q_s = Q, \quad \text{for } y \text{ components,}$$

$$Q_x = X h_x = M_x, \quad \text{for moments,}$$

which yield

$$Q_s = Q - \frac{M_x}{h_x} (\tan \theta_0 + \tan \theta_u) \quad (19)$$

or

$$Q_s = \frac{Q}{h_x} [h_x - x (\tan \theta_0 + \tan \theta_u)] = Q \frac{h_{0x}}{h_x} \quad (19a)$$

As shear stress  $\tau$  in the web, we have

$$\tau = \frac{Q_s}{h_x s} = \frac{Q}{s} \frac{h_{0x}}{h_x^2} \quad (19b)$$

If the spars in a girder are not parallel the cross stress in the web can become higher, lower, or even inversely directed to the outside cross stress, according to the spar setting. The ratio  $Q_s/Q$  being solely affected by that of the girder height at both points, but not on the angle of setting of both spars to each other, the difference between  $Q_s$  and  $Q$  remains, even if the spars are only slightly inclined, when only the height of the girder decreases, as in the wing spars of an airplane.

Now we calculate the tension stresses in an infinitely thin web plate (diagonal tension field) with spars not set parallel (Fig. 15). For simplification we assume the spars straight and  $\vartheta_o = \vartheta_u = \vartheta$ , so that the uprights are perpendicular to the mean direction of both spars (i.e., perpendicular to their angular symmetry); other similar cases can be treated as in Part I of this report (N.A.C.A. Technical Memorandum No. 604). We consider only the case that the cross stress within the scope of our discussion of the plate wall is constant. Lastly, we suppose the dimensions of the girder to be such that the direction of the tension stresses (wrinkles) is constant within the entire scope of examination of the web plate ( $\alpha = \text{constant}$ ).

It becomes apparent from equation (19b) that the shear stresses in the web under shear vary in the x-direction even when the cross stress  $Q$  is constant. Consequently, the tension stresses will be of different magnitude in different parts of the web plate even by the diagonal tension field. But from the as-

sumedly constant direction of the wrinkles and from the freedom of sources in the field of the principal stresses (See Part I - N.A.C.A. Technical Memorandum No. 604, theorem 2, page 11), it follows that the tension stresses are constant along every stress trajectory (wrinkle).

The exact treatment of the problem yields an integral equation which we shall omit here, and simply give an approximation which is sufficiently accurate for all practical purposes. We assume that the tension stresses  $\sigma_m$  in the middle of the girder (that is, on axis  $x$ ) correspond to the shear stresses, according to (19b), so that (Compare Figure 15 and equation (9) (Part I - Technical Memorandum No. 604, page 25) )

$$\sigma_m = \frac{Q}{s} \frac{h_{QX}}{h_x^2} \frac{1}{\sin \alpha \cos \alpha} = \frac{Q_s}{h_x s} \frac{1}{\sin \alpha \cos \alpha} \quad (20)$$

In conformity with this assumption the tension stresses in the whole field are now known, inasmuch as they are constant along every stress trajectory. So, for example, the tension stress in the web plate in point O at the upper spar at point  $x$  is just as high as in point  $P_1$ , which lies on axis  $x$  at point  $x - \frac{1}{2} h_x \cot \alpha$ . The tension stress at this point is (Compare equation (20))

$$\sigma_{m1} = \sigma_o = \frac{Q}{s} \frac{h_{QX}}{h_1^2} \frac{1}{\sin \alpha \cos \alpha} = \sigma_m \frac{h_x^2}{h_1^2}$$

and with

$$h_1 = h_x - 2 \frac{h_x}{2} \cot \alpha \tan \vartheta,$$

we obtain

$$\sigma_U = \sigma_m \frac{h_x^2}{h_1^2} = \sigma_m \frac{1}{(1 - \cot \alpha \tan \phi)^2} \quad (20a)$$

which, applied to point U, yields

$$\sigma_U = \sigma_m \frac{h_x^2}{h_2^2} = \sigma_m \frac{1}{(1 + \cot \alpha \tan \phi)^2} \quad (20b)$$

Thus it becomes apparent that the tension stresses are not uniformly distributed over the cross-sectional height; it is higher in the upper than in the lower portion of the cross section.

Now to check the calculation we examine the equilibrium on an upright. The stress exerted by the upper spar on the upright due to the stressed skin is (See Figure 16):

$$- V_O = Z (\sin \alpha - \cos \alpha \tan \phi).$$

Hereby,  $Z = \sigma_O s t (\sin \alpha - \cos \alpha \tan \phi)$ ,

consequently,  $- V_O = \sigma_O s t (\sin \alpha - \cos \alpha \tan \phi)^2$ .

For  $\sigma_O$ , in itself variable over the width  $t$ , we use the approximate value  $\sigma_O$  (according to equation (20a)) at the point of attachment of the upright, which inserted, reads as

$$- V_O = \sigma_m s t \sin^2 \alpha.$$

For  $V_U$  we obviously obtain the same value. Our check is correct  $V_O = V_U = V$  and yields with (20)

$$- V = Q_S \frac{t}{h_x} \tan \alpha \quad (20c)$$

## Introduction of Outside Stresses

A discussion of stress distribution in a sheet metal girder at the point of introduction of outside stresses is beyond the scope of this paper, and we shall merely point out several features.

If a stress (Fig. 17) is applied at the end of a sheet metal girder, the end member must be resistant to bending in order to be able to take up the laterally acting stress component of the skin stress. In relatively high girders this is easily accomplished and it is best, as shown on Figure 17, to stiffen the panel between the first two uprights by special reinforcements and then assume that the tension stresses to the right of this panel are uniformly distributed across the web plate.

Applying stress  $Q$  at any other central upright (instead of at the end of the girder) which is neither resistant nor rigid in bending, then the sheet wall (Fig. 18) prevents the member from lateral deflection, which then is subjected to tension stresses even in the initially unstressed part of the girder (left of  $Q$ , Fig. 18). In the stressed portion (at right of  $Q$ , Fig. 18), the tension stresses in the web are evenly distributed near the point where  $Q$  is applied. If the girder dimension is conformal to this loading, it will be advisable to make the web at this point slightly stronger than the even tension stress distribution would call for.

Applying stress  $Q$  at an upright in the middle of the girder  $Q$  distributed over both sides (Fig. 19) and the size of the upright at which  $Q$  is applied, such as to assure the same compression stress in every point (Fig. 19, cross-sectional area increasing upward), we can presume the distribution of the tension stresses in the web plate to be uniform, even if the upright is not rigid in bending.

Now we discuss the case of cross stresses acting on every upright (disregarding exceptional cases). We assume the dimension of the sheet metal girder such that the direction of the tension stresses is constant anywhere in the web plate. While making this assumption, we shall discuss two specific limiting cases, that is, the case of uprights perfectly rigid in bending and that of uprights without any rigidity in bending.

In uprights perfectly rigid in bending, which are pin-jointed to the spars (Fig. 20), the tension stresses in the web are constant in every panel lying between two uprights. If  $Q_L$  and  $Q_R$  denote the cross stresses to be taken up by the girder in the right and left panel of the upright (that is,  $Q_R = Q_L + P_n$ ), the web tension stresses in these two panels are (Compare equation (9), Part I - Technical Memorandum No. 604):

$$\sigma_L = \frac{Q_L}{hs} \frac{1}{\sin \alpha \cos \alpha}; \quad \sigma_R = \frac{Q_R}{hs} \frac{1}{\sin \alpha \cos \alpha}.$$

Stress  $V$  in the upright varies over its length; it is higher by  $P_n$  at the upper end ( $V_0$ ) than at the lower end; stress

$P_n$  is evenly initiated in the web (because  $\sigma_R$  is greater by a constant amount than  $\sigma_L$ ).

Now the stress in the upright is:

$$- V_m = \frac{Q_R + Q_L}{2} \frac{t}{h} \cot \alpha + \frac{P_n}{2}, \quad \text{at center}$$

$$- V_0 = - V_m + \frac{P_n}{2}, \quad \text{at top}$$

$$- V = - V_m - \frac{P_n}{2}, \quad \text{at bottom}$$

These equations are easily extended to the case where  $P_n$  is applied at the bottom instead of at the top or where  $P_n$  acts upward instead of downward.

The case of uprights without rigidity in bending (Fig. 21) which approaches actual conditions much more closely than the one discussed here can, by constant direction of the wrinkles, be debated only with the assumption that the outside stress on every upright (at least within the scope of our consideration) by constant spacing of uprights is equivalent (respectively proportional to this spacing when the spacing varies). When, as supposed, the direction of the tension stress on the upright does not change and there is no lateral stress, the intensity of the tension stress is likewise unchangeable. The tension stresses  $\sigma$  proceed undisturbed beyond the upright; they are constant along every stress trajectory.

But now the tension stresses continue (in contrast to the case above) to increase upward and downward, and from left to

right, respectively. Now the stress in every upright is constant over its length.

Again, using our previous symbols  $Q_L$  and  $Q_R$ , and expressing the tension stresses in the web by  $\sigma_O$ ,  $\sigma_U$ ,  $\sigma_m$ , (Fig. 21), we compute

$$\sigma_m = \frac{Q_L + Q_R}{2} \frac{1}{hs} \frac{1}{\sin \alpha \cos \alpha},$$

$$\sigma_O = \sigma_m - \frac{1}{2} \frac{P_n}{ts} \frac{1}{\sin^2 \alpha},$$

$$\sigma_U = \sigma_m + \frac{1}{2} \frac{P_n}{ts} \frac{1}{\sin^2 \alpha},$$

$$V = \frac{Q_L + Q_R}{2} \frac{t}{h} \tan \alpha + \frac{P_n}{2}.$$

#### The Stress in Uprights - Eccentrically Arranged Uprights

In Part I we analyzed the stress in the upright of a sheet metal girder whose web plate formed a diagonal tension field. Now we discuss the resistivity of an upright against this stress; foremost we shall consider the effect of the stressed skin on its buckling strength.

Take a sheet metal girder with a very thin-walled web plate (Fig. 22) and having uprights whose spacing  $t$  is very narrow with respect to the height  $h$  of the girder. These uprights are to be arranged on one side of the plate wall only, so that the stress initiated by the spar on the upright, due to the

stressed skin becomes eccentric. The result of this eccentric compression is bending stresses in the upright, which bulges and carries the web, fastened to it, along with it.

Now let us discuss the general case where the cross-sectional area  $F_y$  of the upright as well as the distance  $e$  of its C.G. from the plane of the plate, and its inertia moment  $J_y$ , varies along the length of the upright. But at the same time we assume that these cross-sectional quantities of the uprights are identical for all others within the scope of the sheet wall in question, so that the elastic line of all these eccentrically stressed uprights is the same.

To define the stress we now envisage a separate piece of the sheet wall of width  $t$  and height  $\Delta y$  and symmetric to the upright, together with the corresponding part of the upright. The inside stresses acting at the intersections of this wall element are applied as outside stresses and we analyze its equilibrium.

First, we have the stresses exerted by the surrounding sheet on the sheet element, which we divide into shear acting along the section edges and normal stress perpendicular to the edges, as illustrated by Figure 22. It becomes apparent that these stresses are in equilibrium with respect to direction  $x$  as well as direction  $y$ . Components perpendicular to the initial plane of the sheet have only the two shear stresses acting on sections II (the components of these two stresses are inversely equivalent, hence compensate each other) and the two normal stresses

acting at I. The intensity of these normal stresses is  $V$  ( $-V$  denoting the force in the upright). The sum of their components perpendicular to the plane of the sheet is  $V \Delta \varphi$ , when  $I$  is the angle between the two tangents in the direction of the upright to the surface of the sheet wall in both intersections.

Since, however, the totality of all stresses acting on the wall element must be in equilibrium, the two stresses disregarded thus far and which themselves are transmitted at the intersections of the upright (these forces are  $-V$ ) must have as resultant an inversely equivalent component perpendicular to the initial plane of the sheet. Thus it follows that these two stresses must also form angle  $\Delta \varphi$ , that is, form the same angle  $\delta$  (Fig. 22) at their points of application with the curved surface of the sheet. This being valid for all possible intersections, we have theorem 3: The angle of the curved line of action of the stress in the upright with the curved surface of the web plate is constant along the entire length of the upright. This is even applicable, in general, to uprights with variable inertia moment and eccentricity in length.

Now let us consider the special case of uprights not restrained at the end (Fig. 23). Owing to the movement of the web out of its initial plane the stress exerted by the web on the spar is no longer in the initial plane of the wall, but moves along with the wall. So the stress of the spar at the attachment of the upright acts in the tangential plane on the

wall. Its angle with the wall and its distance from it is zero. This being valid for upper and lower end of the upright, the curve of action of stress  $-V$  must act along the entire member with the wall. From this it follows - even for variable eccentricity  $e$  - that the bending moment  $M_y$  in the upright is

$$M_y = V e \quad (21)$$

So, while the eccentricity of a member merely stressed in buckling by the eccentrically acting stresses increases in the middle as the stress increases, that of the uprights lying within the sheet wall is not affected by the intensity of the stress. Such uprights, very closely spaced in the wall, surely will not buckle as long as the assumption of equal elastic line for all members holds true; consequently, their calculation is very simple. They merely must be dimensioned for eccentric compression, whereby the resultant stress in compression and bending must not exceed the yield limit of the material, respectively, that stress in compression which induces wrinkling.

Now, we consider the case (Fig. 23) where the ends of the uprights are more or less constrained and have constant cross-sectional dimensions. Conformally with theorem 3, the differential equation for the elastic line of the upright ( $\xi$  = deflection of upright at point  $y$ ) reads:

$$\frac{d^2 \xi}{dy^2} = \frac{1}{E J_y} \left( M_0 + \frac{d H}{d y} y \right) \quad (22a)$$

The two constants  $M_0$  and  $\frac{dM}{dy}$  characterize the moments and may, in given cases, be considered as defining constants of integration. The solution with constants  $A$  and  $B$  yields

$$y = A + B y + \frac{y^2}{2} \frac{V e}{E J_V} \left( M_0 + \frac{1}{3} \frac{dM}{dy} \right) \quad (22b)$$

In the particular case where the upright is perfectly constrained at the bottom ( $y = 0$ ), but not at the top ( $y = l$ ), the four limiting equations become:

$$\zeta = 0; \quad \frac{d\zeta}{dy} = 0, \quad \text{for } y = 0$$

$$\zeta = 0; \quad \frac{d\zeta}{dy} = \frac{V e}{E J_V}, \quad \text{for } y = l.$$

The moment  $M_0$  at the point of constraint is

$$M_0 = -\frac{1}{2} V e$$

and at  $y$

$$M = -\frac{1}{2} V e \left( 1 - 3 \frac{y}{l} \right)$$

The elastic line and the moments are shown in Figure 23.

If the upright is perfectly constrained at both ends and the cross section is constant, then the moment along the whole member is zero.

Thus far we have treated very (infinitely) closely spaced uprights, but the conditions become somewhat different when these members are spaced farther apart. In Figure 22, in particular, bending moment  $M$  is higher in the middle (that is, from  $y = t \tan \alpha$  to  $y = h - t \tan \alpha$ ) than at the ends, even by constant

inertia moment  $J_V$  in the uprights, so that (without giving the derivation)

$$M = V e \frac{1}{1 - V \frac{t^2 \tan^2 \alpha}{12 E J_V}} \quad (23)$$

This hinges on the condition that the normal stress acting at section I (Fig. 23), which represents the resultant of all normal stresses applied at this section, is slightly closer to the initial plane of the sheet metal by wider spacing than the sheet itself on the upright. Because, when the uprights are spaced farther apart the portions of the sheet - after deformation - more in the middle between two uprights, are a little closer to the initial plane of the sheet than these portions on the uprights.

The validity of (23) extends to  $0 \leq \tan \alpha \leq \frac{h}{2}$ . The apparent increase in eccentricity raises, as we see, with the stress. The buckling load derived from this formula (23) is

$$V = \frac{12 E J_V}{t^2 \tan^2 \alpha} \quad (23a)$$

(We refer to this again in the following section.)

The results are exactly similar for oblique uprights. They also show that the bending moment is  $M = V e$ , etc. by very narrow spacing.

## The Theoretical Buckling Load of Uprights

This section is confined to the purely theoretical problem of buckling in uprights, while the next section treats the wrinkling phenomena.

To simplify matters we limit ourselves to sheet metal girders with uprights perpendicular to the spars, after which the results are easily applied to oblique members (Compare Figure 23).

When an upright buckles from the original plane of the wall, the web plate must, perforce, do likewise. The web, stressed in tension, buckles at the upright and exerts a side load  $p$  (due to deflection in tension) on it, which endeavors to force it back to its original position. (This load  $p$  increases directly proportional to the deflection of the uprights, thus effecting a higher buckling load  $V$ .)

The elastic line of a compressed and simultaneously laterally stressed member complies with the well-known

$$\frac{d^4 \zeta}{dy^4} + \frac{V}{E J_V} \frac{d^2 \zeta}{dy^2} = \frac{p}{E J_V} \quad (24a)$$

(See foregoing section for explanation of symbols.)

In the following we assume the inertia moment  $J_V$  constant and of equal magnitude.

We now compute the side load  $p$ .  $Z$  is the tension in a strip of the skin, crossing the length  $l$ , of the upright;  
 $Z = l \cos \alpha \sigma s$ . So, in conformity with equations (9) and (10), we have:

$$Z = V \frac{h \cot \alpha}{t} \frac{1}{\sin \alpha} .$$

This tension  $Z$  is now turned at angle  $\Delta$  (Compare, for example, Figures 24 and 25), so that  $p = Z \Delta$ . Inserted in equation (24a) it yields

$$\frac{d^4 \zeta}{dy^4} + \frac{V}{E J_V} \frac{d^2 \zeta}{dy^2} = \frac{V}{E J_V} \zeta \frac{\Delta}{\zeta \sin \alpha} \frac{h \cot \alpha}{t} \quad (24b)$$

As a rule,  $\Delta$  varies over the length of the upright, and depends, in particular, on its spacing.

#### Discussion of Various Special Cases

##### Case 1, $t \geq h \cot \alpha$ .

Here every tension diagonal crosses only one vertical member. The size of angle  $\Delta$  of the tension diagonal becomes apparent from Figure 24. We obtain

$$\frac{\Delta}{\zeta \sin \alpha} = \frac{1}{\zeta \sin \alpha} \left[ \frac{\zeta}{y} \frac{1}{\sin \alpha} + \frac{\zeta}{h-y} \frac{1}{\sin \alpha} \right] = \frac{h}{y(h-y)} .$$

We write this value in (24b), resolve this equation\* and obtain as theoretical buckling load  $V_T$

$$V_T = P_E \frac{1}{1 - 0.49 \frac{h \cot \alpha}{t}} \quad (24c)$$

---

\*In these and subsequent differential equations, we represented the elastic line of the upright by Fourier series. The finite number of terms assumed in the calculation makes the buckling loads only approximately correct, although the error amounts to only a very small per cent.

for uprights not restrained at the end;

$$V_T = 4 P_E \frac{1}{1 - 0.33 \frac{h \cot \alpha}{t}} \quad (24d)$$

for uprights rigidly restrained.

Here  $P_E$  is Euler's buckling load of the second order, so

$$P_E = \pi^2 \frac{E J_y}{h^2} \quad (24e)$$

All uprights have the same elastic line when buckling. If  $h \cot \alpha/t$  is very high, the buckling load changes into Euler's load.

Case 2,  $t = \frac{1}{2} h \cot \alpha$ .

In this case every tension diagonal crosses two uprights.

( $\Delta$  is read from Figure 25.) We obtain

$$\frac{\Delta}{\zeta \sin \alpha} = \frac{1}{\zeta \sin \alpha} \left[ \frac{\zeta}{\sin \alpha} - \frac{\zeta_1 - \zeta}{\frac{h}{2 \sin \alpha}} \right] = \frac{1}{y} + \frac{2}{h} \left( 1 - \frac{\zeta_1}{\zeta} \right) \quad (24f)$$

where  $\zeta_1$  is the deflection of the adjacent upright at point  $y + h/2$ . Now we continue our calculation under the two assumptions:

Assumption a) While bulging, the elastic line of two adjacent uprights is inversely equivalent. In this case we must set  $\zeta_1$  in (24f) equivalent to the negative deflection of the considered upright, even at point  $y + h/2$ . Written in (24b) the theoretical buckling load  $V_T$  becomes:

$$V_T = 5.3 P_E \quad (24g)$$

for uprights not constrained;

$$V_T = 8.8 P_E \quad (24h)$$

for uprights rigidly constrained.

The elastic lines are as shown in Figure 25; every member forms two waves when bulging.

Assumption b) All uprights have the same elastic line when bulging. Then  $\xi_1$  is at the same time the deflection in the considered upright even at point  $y + h/2$ . So, when we write (24f) in (24b), we obtain as theoretical buckling load:

$$V_T = 5.3 P_E \quad (24i)$$

for uprights not restrained;

$$V_T = 9.7 P_E \quad (24k)$$

for uprights rigidly constrained.

The elastic line in this type of buckling shows only one wave (Fig. 25b). Thus we see both assumptions accidentally yield identically high buckling loads for this particular spacing of unrestrained uprights.

Now it becomes apparent that all uprights have the same elastic line (one wave) by wider spacing ( $t > \frac{1}{2} h \cot \alpha$ ) and adjacent uprights have different elastic lines (two waves) when spaced close together ( $t < \frac{1}{2} h \cot \alpha$ ). The change-over occurs at precisely  $t = \frac{1}{2} h \cot \alpha$ .

Only one wave occurs at  $t = \frac{1}{2} h \cot \alpha$  when the uprights are constrained (the same elastic line), because this type of deformation is induced by a lower buckling load.

Case 3, Limiting case  $t \rightarrow 0$ .

Here the uprights are very (infinitely) close together.

Assumption a) All uprights have different elastic lines.

Axis  $x$  is placed parallel to the spar, axis  $y$  as before, in the direction of the uprights, and  $\zeta = \zeta(x,y)$  is the deflection of the uprights. In this case of infinitely close uprights  $\zeta(x,y)$  represents at the same time the surface (for it is connected to the uprights) into which the web changes when buckling.

Here it is perhaps more appropriate to speak of bulging of the plate wall (web) instead of bulging of the uprights; the whole web forms oblique wrinkles (like a sheet in wrinkling under shear).

Denoting with  $dz$  a linear component in the direction of tension  $\sigma$ , then  $\frac{\partial \zeta}{\partial z} = \zeta'$  is the angle of the tension diagonal due to bulging and the original plane of the wall. As seen from Figure 26, angle  $\Delta$ , at which the tension is deflected when bulging, is of the order of

$$\Delta = \frac{\partial^2 \zeta'}{\partial z^2} \frac{t}{\cos \alpha} = \frac{\partial^2 \zeta}{\partial z^2} \frac{t}{\cos \alpha}$$

We note that

$$\frac{dx}{dz} = \cos \alpha, \quad \frac{dy}{dz} = \sin \alpha,$$

that, in fact,

$$\frac{\partial^2 \zeta}{\partial z^2} = \frac{\partial^2 \zeta}{\partial x^2} \cos^2 \alpha + 2 \frac{\partial^2 \zeta}{\partial x \partial y} \sin \alpha \cos \alpha + \frac{\partial^2 \zeta}{\partial y^2} \sin^2 \alpha$$

according to the rules of the partial differentiation. Now we write this value for  $\Delta$  into (24b) (including the partial differentiation), and obtain

$$\frac{\partial^4 \zeta}{\partial y^4} = \frac{V}{E J_V} \left[ \frac{\partial^2 \zeta}{\partial (x \tan \alpha)^2} + 2 \frac{\partial^2 \zeta}{\partial y \partial (x \tan \alpha)} \right] \quad (24l)$$

This equation is, of course, fulfilled when  $\zeta(x, y) = 0$ . But, as in every simple problem of buckling, the question is to find those values of  $\frac{V}{E J_V}$ , at which this differential equation yields a solution for  $\zeta \neq 0$ .

In the selection of limiting conditions we must observe: That the calculation is based on the assumedly different elastic lines of the uprights. Thus, if the spar is not rigid in torsion (and the ends of the uprights are not restrained), the elastic lines of the individual vertical members may assume a different angle of slope on the spar without the distortionless spar offering any resistance against this reciprocal distortion of its cross sections. On the other hand, if the spar is rigid in torsion (provided, of course, the vertical members are rigidly attached to the spar), it offers some resistance against distortion, and, if very highly torsion-resistant, finally forces the elastic lines of all uprights into the same angle of slope as the original plane of the sheet. This raises the re-

sistivity of the plate wall against bulging.

Moreover, we stress at this point that there is an exact buckling load even for eccentrically arranged uprights, that is, (by equal distortion stiffness of the spars) exactly the same buckling load as in centrally arranged uprights. (This applies to very (infinitely) closely spaced uprights. For different spacing, particularly by  $t > \frac{1}{2} h \cot \alpha$  there is no pure buckling load in eccentrically arranged uprights; the conditions then are similar to those in the conventional, eccentrically loaded buckling members.)

If, for example,  $\zeta_I = \zeta_I(x, y)$  is the solution of (241) for centric uprights with torsion-resistant spars ( $\zeta_I$  complies with  $\frac{\partial \zeta}{\partial y} = 0$  at upper and lower spar), then  $\zeta_{II} = \zeta_I + a_0 + a_1 y + a_2 y^2 + a_3 y^3$  is likewise a solution of this equation. But by appropriate choice of constants  $a \neq 0$ ,  $\zeta_{II}$  now satisfies  $\frac{\partial \zeta}{\partial y} = \text{constant}$  for upper and lower spar. In this manner the solution conforms to the case of torsion-resistant spars, which, due to the eccentric uprights, twist at a constant angle over their whole length under loading (Fig. 22). The case of perfectly torsion-resistant spars with eccentric uprights is, of course, identical with that of rigidly restrained uprights.

Dr. Schmieden, Danzig, made an accurate solution of (241) which he intends to discuss at some other time. We simply state his results.

The buckling load of the upright is

$$V_T = 7.01 P_E \quad (24m)$$

for unrestrained uprights or spars not resistant to distortion

$$V_T = 11.43 P_E \quad (24n)$$

for perfectly restrained uprights or perfectly distortion-resistant spars, regardless of whether the vertical members are stressed centrally or eccentrically.

Assumption b) All uprights have the same elastic line. The buckling load is:

$$V_T = 13 \left( \frac{h \cot \alpha}{t} \right)^2 P_E \quad (24o)$$

for restrained and unrestrained uprights.

As seen from Figure 27, this equation yields the buckling load for unrestrained uprights with completely torsion-resistant spars; because the above assumption yields for this case the lowest possible buckling load.

The results of all these calculations have been tabulated in Figure 27, namely;

AB applies to eccentric or centric uprights rigidly restrained or rigidly attached to distortion resistant spars;

BC applies to centric, rigidly restrained uprights;

BF applies to centric, unrestrained uprights, rigidly attached to distortion-resistant spars;

DF is valid for centric or eccentrically arranged, but unrestrained uprights with spars not resistant to distortion;

FG applies to centrically arranged, nonrestrained uprights.

The Figures 24c to 24n denote the respective equations by which the dotted portions of the curves and the points enclosed by a small circle were computed. (The computed portions of the curves which do not check with the final curves are shown as dotted lines.)

Of course, there is no such thing as a perfectly rigid restraint in uprights, nor perfectly distortion-resistant spars. But the rigidity of restraint technically obtainable has, as a rule, relatively little effect on the buckling strength of vertical members. For that reason it is advisable to stay on the safe side and to use only the lowest curves of Figure 27.

If some uprights are stronger than others near by or braced perpendicular to the plane of the sheet wall, the buckling strength of the latter is naturally augmented.

#### The Actual Buckling Load; Index Value\*

This section pertains to uprights symmetrically attached to the web plate.

In the last section we treated the theoretical buckling stress of uprights without consideration of wrinkling phenomena

---

\*It is assumed that the reader is familiar with my report, "Remarks on Buckling Members; Index Value," Zeitschrift für Flugtechnik und Motorluftschiffahrt, 1928, p. 241.

or excess of yield limit. So in the following we shall show how to dimension the vertical member when the buckling strength of unrestrained free buckling members of corresponding cross-sectional shape is known (as from tests, for instance). By "free" buckling struts we mean here the conventional type, that is, without lateral support, in contrast to the vertical members of a sheet metal wall, which we call, for short, "uprights."

For we can assume that the actual buckling load  $V$  of an upright of length  $h$ , even when wrinkling and excess of yield limit is taken into account, is just as high as that of a free buckling member with the same cross-sectional form and area (hence, of equal actual buckling stress  $\sigma$ ) by so selecting the length  $l_1$ , of this free buckling member that both members have the same theoretical buckling load  $V_T$ ; that, in consequence (Compare (24e)):

$$\frac{\pi^2 E J}{l_1^3} = V_T = P_E \frac{V_T}{P_E} = \frac{\pi^2 E J}{h^3} \frac{V_T}{P_E}$$

A comparison of the left with the right side of this formula now yields the length of this "equivalent" free buckling member at

$$l_1 = h \sqrt{\frac{P_E}{V_T}} \quad (25)$$

In this manner we reduce the problem of the dimension of the upright to that for this "equivalent" free buckling member of length  $l_1$ , and to the (actual) buckling load  $V$ .

The profile shape and the allowable stress of this "equiva-

lent" free member with index value

$$K = \frac{\sqrt{V}}{l_1} = \frac{\sqrt{V}}{h} \sqrt{\frac{V_T}{P_E}}$$

is best taken from the index-stress-strain diagram (Compare Zeitschrift für Flugtechnik und Motorluftschiffahrt, 1928, page 342). Bearing in mind formula (10) this index can also be expressed\* as

$$\begin{aligned} K &= \frac{\sqrt{Q}}{h} \sqrt{\frac{t}{h \cot \alpha}} \sqrt{\frac{V_T}{P_E}} = \\ &= K_W \sqrt{\frac{t}{h \cot \alpha}} \sqrt{\frac{V_T}{P_E}} = K_W \frac{K}{K_W} \end{aligned} \quad (26)$$

We note that  $\frac{V_T}{P_E}$  with respect to  $\frac{t}{h \cot \alpha}$  is known (Fig. 27), and plot  $\frac{K}{K_W}$  against  $\frac{t}{h \cot \alpha}$ , as in Figure 28. By equal girder height  $h$  and equal cross stress  $Q$  the index value  $K$  for the uprights of a sheet wall girder is always higher than the index value

$$K_W = \sqrt{Q/h}$$

for the uprights of a trussed girder, provided, the uprights of the former are spaced farther apart than  $\frac{1}{6} h \cot \alpha$ . A higher index value, however, denotes higher allowable stress.

By virtue of the closer spacing of the uprights and the ensuing reduced buckling length of the spars, those of a sheet metal girder can always be subjected to higher stresses than those of a trussed girder. And this is the reason a correctly

constructed sheet metal girder is always lighter than a trussed

\* $K_W$  is the index value for the sheet metal girder (Compare Part I, N.A.C.A. Technical Memorandum No. 604); at the same time it is the index value for the uprights of a trussed girder by equal cross stress  $Q$  and girder height  $h$ .

girder; and it applies, in particular, to girders stressed in both directions (alternating) by cross stresses. For sheet metal girders need merely be constructed for the higher of the two stresses, while a trussed girder must be reinforced by crossed tension diagonals, unless the diagonal is resistant to compression; both constitute an increase in weight.

#### E x a m p l e

Height of girder,  $h = 80$  cm; spacing of uprights,  $t = 25$  cm; wrinkles at  $\alpha = 45^\circ$ ; cross stress,  $Q = 10,000$  kg. The uprights, which are to be unrestrained, are of the shape shown in Figure 29.

What are the dimensions of these uprights? With  $t : h \cot \alpha = 25 : 80 = 0.313$ , Figure 28 yields  $\frac{K}{K_W} = 1.43$ . Consequently (Compare equation (23))

$$K = K_W \frac{K}{K_W} = \frac{\sqrt{10000}}{80} \times 1.43 = 1.78.$$

For this index value, Figure 29 gives the allowable stress  $\sigma = 2650$  and the wall thickness ratio of the profiles as  $a/s = \sim 12$ . With a stress in the upright of  $V = Q \frac{t}{h \cot \alpha} = 10000 \times 0.313 = 3130$ , we select from our table a section with a cross-sectional area of  $F_V = V/\sigma = 3130 : 2650 = 1.2 \text{ cm}^2$  and a wall thickness ratio of  $a/s = \sim 12$ .

But we have ignored as yet the web between the two pieces forming the profile of the upright, which likewise contributes

to the cross section of the upright. The allowable stress is found as follows: Let  $F_P$  be the cross section of both profiles alone, and  $F_B$  that of the stressed skin. Then we assume the actual buckling stress  $\sigma$  (inclusive of wrinkling and exceeding the yield limit) of the profile with enclosed skin portion to be precisely as high as that of the identical profiles without this skin portion, when we so choose the length ratios of both members that both offer the same safety with respect to theoretical buckling load under buckling stress  $\sigma$ .

First we compare two free buckling members:

	
$F = F_P + F_B$	$F_1 = F_P$
$\sigma$	$\sigma_1 = \sigma$
$V = (F_P + F_B)\sigma$	$V_1 = F_P\sigma = V \frac{F_P}{F_P + F_B}$
$J$	$J_1 = J$
$P_E = \pi^2 \frac{E J}{l^2}$	$P_{E_1} = (\text{according to assumption}) P_E \frac{V_1}{V} =$
	$= \pi^2 \frac{E J}{l^2} \frac{F_P}{F_P + F_B} = \pi^2 \frac{E J}{l_1^2}$

consequently,

$$l_1 = \sqrt{\frac{F_P + F_B}{F_P}} l$$

$$K = \frac{\sqrt{V}}{l} \quad K_1 = \frac{\sqrt{V_1}}{l_1} = \frac{\sqrt{V}}{l} \left( \sqrt{\frac{F_P}{F_P + F_B}} \right) = K \frac{F_P}{F_P + F_B}$$

Applied to the upright of the sheet metal wall, the index value (Note formula (26)) becomes

$$K_1 = \frac{F_P}{F_P + F_B} K = \frac{F_P}{F_P + F_B} K_W \frac{K}{K_W} \quad (27)$$

Since  $F_P$  itself depends upon the allowable stress for a given stress in the upright, we first estimate  $\sigma$  and  $F_P$ , then define  $K_1$  and finally determine  $\sigma$  and  $F_P$  from this value.

#### E x a m p l e

We use the figures of the preceding example and further assume <sup>a</sup> 0.7 mm skin covering (equivalent to a 3560 stress in tension). We estimate the width of the stressed skin at 100 s, so that  $F_B = 100 s^2 = 0.49 \text{ cm}^2$ . With an allowable stress of 2300 (estimated) we have:  $F_B + F_P = \frac{V}{\sigma} = 3130 : 2300 = 1.36 \text{ cm}^2$ , and (Compare figure of preceding example and formula (27)):

$$K_1 = \frac{1.36 - 0.49}{1.36} 1.78 = 1.14.$$

Now the allowable stress, according to Figure 29, is  $\sigma = 2340$ ; further  $a/s = 15$ ; hence  $F_V = \frac{V}{\sigma} = 3130 : 2340 = 1.40$ ;  $F_P = 1.40 - 0.49 = 0.91 \text{ cm}^2$ . The saving here amounts to 25% compared to the preceding example.

For  $K_W = \frac{\sqrt{Q}}{h} = 1.25$ , Figure 29 yields  $\sigma = 2320$  as the allowable stress for the upright of a trussed girder; the cross-sectional area of this member is  $\frac{Q}{\sigma} = 10000 : 2320 = 4.3 \text{ cm}^2$  and (with a diagonal set at  $45^\circ$ ) compared to the sheet metal wall at  $t = 25 \text{ cm} : 4.3 \times \frac{25}{80} = 1.34 \text{ cm}^2$ . The saving in weight in the uprights of the sheet metal wall is 32 per cent compared to that in the trussed girder.

When the web plates have relatively thick walls (i.e., by

high index values) it is advisable to space the uprights comparatively close, for in that way it becomes possible to use a large portion of the web plate as cross section for the uprights.

### The Transition $s \rightarrow 0$

Deviations from the Simple Theory when Plate Thickness is Finite

#### Wall Component

First we discuss the permissible omissions in the stress calculation of web plates (of a sheet metal girder) when changing from plates with infinite thickness to such with finite thickness.

Let us consider the component of a plate wall shown on Figure 30, where

- $s$  = wall thickness of web plate,
- $b$  = width of a half wrinkle,
- $f$  = depth of a wrinkle,
- $m$  = transverse contraction factor (for example,  $m = 3.3$ )\*
- $\sigma$  = principal stress acting in direction of the wrinkles,
- $-\sigma_{qk}$  = compression stress acting transverse to the direction of the wrinkles,
- $\alpha_E = \frac{1}{E}$  = elongation factor.

The resistance to wrinkling of a plate of finite thickness, must balance (since we disregard the presence of outside stresses perpendicular to the plate) the compression stresses  $\sigma_{qk}$  acting on edges A. Euler's buckling formula yields these compression

\*For simplification, we set  $1 - 1/m^2 = \sim 1$ .

stresses as

$$- \sigma_{qk} = \frac{\pi^2}{12} E \left( \frac{s}{b} \right)^2 \quad (28)$$

Their intensity is (with infinitely small error) unaffected by the depth of the wrinkles and (conformal to assumption

1. -  $\frac{1}{m^2} = \sim 1$ ) by the presence of tension stress  $\sigma$ .

Now we calculate the depth of the wrinkles for a given transverse contraction  $-\epsilon_q$ , which like the approach of both edges A is due to

- 1) the (negative) elongation  $\epsilon_{qk}$  caused by the compression stress  $-\sigma_{qk}$ ,
- 2) the transverse contraction induced by the tension stress  $\sigma$ , and
- 3) the sinusoidal plate wrinkles.

Accordingly, we have for  $-\epsilon_q$

$$-\epsilon_q = -\frac{\sigma_{qk}}{E} + \frac{1}{m} \frac{\sigma}{E} + \frac{\pi^2}{4} \frac{f^2}{b^2} \quad (29)$$

and conformably to equation (28)

$$\begin{aligned} \frac{f}{b} &= \frac{2}{\pi} \sqrt{-\epsilon_q - \frac{1}{m} \frac{\sigma}{E} - \frac{\pi^2}{12} \left( \frac{s}{b} \right)^2} = \\ &= \frac{2}{\pi} \sqrt{-\epsilon_q - \frac{1}{m} \epsilon + \epsilon_{qk}} \quad (29a) \end{aligned}$$

Due to the wrinkles, we have bending stresses in the web plate which attain their maximum in the outer fibers of the plate in the culmination points (or better, culmination lines). These maximum stresses in bending  $\sigma_b$  for a given depth and

width of wrinkles are

$$\sigma_b = \pm \frac{\pi^2}{2} E \frac{s}{b} \frac{f}{b} \quad (30)$$

Before discussing the boundary  $s \rightarrow 0$ , we wish to make several generalized statements regarding infinitely small quantities of the elasticity theory. The elongation factor  $\alpha_E = \frac{1}{E}$  is considered an infinitely small quantity of the first order, so that (by finite  $\sigma$ ) the elongations  $\epsilon = \frac{\sigma}{E}$  are assumed as infinitely small of the first order with respect to the dimensions of the body. Then the buckling stress  $\sigma_k$ , for example, in a buckling member yields, according to Euler's formula

$$\sigma_k = \pi^2 \frac{E}{(l/i)^2} \quad (l/i = \text{degree of fineness})$$

The infinitely large quantity  $E$  of the first order is in the numerator of the right side, so the fineness ratio of buckling members, which buckle according to Euler and thereby show a finite buckling stress  $\sigma_k$ , are rated as infinitely large of the order of  $\frac{1}{2}$ .

Applied to the conditions of a sheet metal wall, it follows that the wall thickness  $\sigma$  of a web plate, which bulges under finite stresses, must be considered as infinitely thin of the order of  $\frac{1}{2}$  with respect to the other dimensions of the plate. For example, the plate thickness of, say, 1 centimeter, in a sheet metal girder with stiffeners (spars) spaced 50 cm apart, must be looked upon as infinitely thin of the order of  $\frac{1}{2}$ . Such

wall thicknesses we call "normally thin."

From equations (28), (29a), and (30) we deduce for normal thicknesses  $s$  (infinitely thin like  $\alpha_E^{1/2}$ ) and for finite width  $b$ , of the wrinkles, the quantities for  $\sigma_{qk}$ ,  $f/b$ ,  $f$ , and  $\sigma_b$ , given in Table II, column 1.

Now we reduce the wall thickness  $s$  still further, that is, from  $\alpha_E^{1/2}$  to  $\alpha_E^{1/2+\kappa}$  ( $\kappa > 0$ ). With width  $b$  of the wrinkle assumed finite, we obtain according to equations (28), (29a), and (30) the order of magnitude for  $\sigma_{qk}$ ,  $f/b$ ,  $f$ , and  $\sigma_b$ , given in column 2 of Table II.

We see, in particular, that  $-\sigma_{qk}$  reaches zero ahead of  $\sigma_b$  when  $s$  is reduced. The ratio of depth to width of wrinkle, that is  $f/b$ , remains infinitely small, as  $\alpha_E^{1/2}$ , as for finite wall thickness, according to (29a), and approaches, by infinitely thin  $s$  within this order of size, the limit value

$$\lim_{s/b \rightarrow 0} f/b = \frac{2}{\pi} \sqrt{-\epsilon_q - \frac{\sigma}{\pi E}} \quad (29b)$$

For later purposes we include the case where the width  $b$  of the wrinkle becomes infinitely small at the same time that the order of magnitude of the wall thickness is reduced as  $\alpha_E^\beta$  ( $\beta > 0$ );  $\beta$  as a rule differs from  $\kappa$ .

TABLE II

	1		2		3	
	infinitely small as		infinitely small as		infinitely small as	
$h^*$	$\alpha_E^0$	finite	$\alpha_E^0$	finite	$\alpha_E^0$	finite
$s$	$\alpha_E^{\frac{1}{2}}$	normally thin	$\alpha_E^{\frac{1}{2}+\kappa}$ ( $\kappa > 0$ )	thin compared to normal	$\alpha_E^{\frac{1}{2}+\kappa}$ ( $\kappa > 0$ )	thin compared to normal
$b$	$\alpha_E^0$	finite	$\alpha_E^0$	finite	$\alpha_E^\beta$ ( $\kappa > \beta > 0$ )	small
$\sigma_{qk}$	$\alpha_E^0$	finite	$\alpha_E^{2\kappa}$	very low	$\alpha_E^{2(\kappa-\beta)}$	very low
$f/b$	$\alpha_E^{\frac{1}{2}}$	normally small	$\alpha_E^{\frac{1}{2}}$	normally small	$\alpha_E^{\frac{1}{2}}$	normally small
$f$	$\alpha_E^{\frac{1}{2}}$	normally small	$\alpha_E^{\frac{1}{2}}$	normally small	$\alpha_E^{\frac{1}{2}+\beta}$	small
$\sigma_b$	$\alpha_E^0$	finite	$\alpha_E^\kappa$	low	$\alpha_E^{\kappa-\beta}$	low, but not very low

\*  $h$  = spacing of reinforcements (uprights and spars, respectively).

If the stresses prevailing during deformation are to be of no higher order than finite (that is, not infinitely high), then  $\kappa$  must be  $\geq \beta$  ( $\sigma_{qk}$  and  $\sigma_b$  become finite for  $\kappa = \beta$ ). The order of magnitude of  $\sigma_{qk}$ ,  $f/b$ ,  $f$ , and  $\sigma_b$  applying to this case, will be found in column 3 of Table II.

Summing up, we find that  $\sigma_{qk}$  is soon negligibly low when the order of magnitude of the wall thickness decreases with respect to the width of the wrinkle; the bending stress  $\sigma_b$  likewise becomes lower (and finally very low), although not quite as rapidly. The ratio  $f/b$  approaches a well-defined limit value of low magnitude.

### The Effect of Attaching the Plate to the Spars

Now we extend our considerations to include the whole sheet wall (Fig. 31). We disregard for the present, the existence of spars and subject the whole sheet to a transverse contraction  $-\epsilon_q$ , by wrinkling it, and apply the tension stresses  $\sigma$  in the direction of the wrinkles. As a result the sheet is lengthened by  $\Delta z$  in the direction of the wrinkles. (The stresses prevalent at these deformations were discussed in the preceding paragraph.)

Now we attach the spars which we set perpendicular to the direction of the wrinkles, that is, parallel to axis  $x$ , in Figure 32. The edges (B in Fig. 31) capable of leaving the original plane of the sheet freely, are now fastened to the spars in such a manner that these edges stay in their initial plane; and, to assume the most unfavorable case, we presume the sheet to be tangentially restrained at these edges.

At first we disregard the disturbances at the edges A and assume the distance  $X$  of these edges to be very great with respect to distance  $h$  of the edges B; and we consider only the stress correspondingly remote from the edges A.

Now it can be shown that the entire form change  $A$ , which the sheet has to take up during all these deformations, is higher than

$$A_{\min} = \frac{1}{2} \left( \frac{\Delta z}{h} \right)^2 E h X s$$

$A_{\min}$  is the work of form change to be taken up by a sheet of given dimensions, when it is merely subjected to a uniform elongation  $\frac{\Delta z}{h}$  in the direction of  $h$ , so the ensuing stresses are simply symmetrical tension stresses  $E \frac{\Delta z}{h}$ .

The difference  $A - A_{\min}$  is due to stresses  $\sigma_{qk}$  and  $\sigma_b$  and to supplementary stresses induced by the rigidity of the edges.

Now we calculate  $A$  for the special case where  $s$  with respect to the size of  $h$  is infinitely thin as  $\alpha_E^{1/2}$ , namely, infinitely thin as  $\alpha_E^{1/2+k}$ . We give this infinitely thin sheet an arbitrary deformation  $A_{\max}$ , which satisfies the edge equations and retains the connection of the sheet at every point. From the theorem of least work of deformation it follows that the work of form change  $A$  of the actually occurring attitude of deformation must be less than that of the arbitrarily chosen, that is,

$$A_{\max} > A > A_{\min} \quad (31)$$

So when we know the work of deformation  $A_{\max}$  of the arbitrarily chosen state of deformation, we have  $A$  confined within two limits. To keep these limits as close as possible the arbitrary deformation is chosen for the least possible work of deformation, that is, as near to  $A_{\min}$  as possible. And now we are able to select a deformation attitude which yields (aside from infinitely small quantities)  $A_{\max} = A_{\min}$ , so that, in consequence,

$$A = A_{\min}.$$

But first we must define the properties of a form change whose work equals  $A_{min}$ , or more exact, which differs from  $A_{min}$  only by infinitely small quantities:

1) The deformations within the whole sheet (aside from infinitely small points) must be such that the stresses of this deformation attitude differs from  $\sigma = \frac{\Delta z}{h} E$  only by infinitely small quantities, or in other words, that

$$\sigma_z = \sigma; \sigma_{qk} = 0; \sigma_b = 0; \tau_{xz} = 0; \text{etc.} \quad (31a)$$

2) Any deviations of finite magnitude from these stresses must be kept to infinitely narrow limits.

One form change which satisfies these conditions is shown in Figure 32. The sheet is evenly wrinkled in the entire middle range, which is  $h - 2r$ , and has within this range the constant elongation  $\frac{\Delta z}{h}$ . Since  $\sigma_{qk}$  and  $\sigma_b$  (respectively, the corresponding elongations) must be infinitely low, the width of the wrinkles must either be chosen as finite or infinitely small of the order of  $\alpha_E^\beta$ , whereby  $\kappa$  must be  $> \beta \geq 0$ . In addition  $f/b$  must be so chosen that equation (29b) is complied with.

At the edges the wrinkles are forced in the plane of the spars; in this upper and lower range of width  $r$  the depth of the wrinkles decreases to zero, that is, less than in the middle. So for a given width of wrinkles and given  $\epsilon_q$ ,  $\sigma_{qk}$  as well as  $\sigma$  (according to (29a)) must differ by a finite amount from zero and  $\frac{1}{E} \frac{\Delta z}{h}$ . Moreover, other additional stresses (such as

shear stresses) of finite magnitude can occur within this range. Hence it is imperative to make this range infinitely small; in fact, we make  $r$  infinitely small as  $\alpha_E^\rho$  ( $\rho > 0$ ).

Now, if  $A_{\max}$  is to equal  $A_{\min}$ , the work of form change  $A_r$  in the infinitely small range of  $r$  must perforce be infinitely small compared to  $A_{\max}$  in the whole web plate;  $\frac{A_r}{A_{\max}}$  must be infinitely small.

Then with the width  $b$  of the wrinkles small as  $\alpha_E^\beta$  (where  $\beta = 0$ , that is, finite width of wrinkles is included in the consideration), and the depth of the wrinkles (according to (29a)) infinitely small as  $\alpha_E^{\frac{1}{2}+\beta}$ , the ratio  $\frac{A_r}{A_{\max}}$  attains the order of  $\alpha_E^{4\beta-3\rho}$ . But this value is infinitely small only when  $4\beta - 3\rho > 0$ , that is, when

$$\beta > \frac{3}{4} \rho \quad (32)$$

But since the range  $r$  must be made infinitely small ( $\rho > 0$ ),  $\beta$  must be made greater than  $0$  ( $\beta > 0$ ) for our arbitrarily chosen deformation, or in other words, we must choose infinitely small width of wrinkles. Then  $A_{\max} = A_{\min}$ .\*

In summarizing, we may say, if  $\alpha_E$  is an infinitely small quantity of the first order, and if  $\kappa$ ,  $\beta$ , and  $\rho$  are figures above zero, and if the plate  $s$  is infinitely thin, as  $\alpha_E^{\frac{1}{2}+\kappa}$ ,

---

\*For  $\rho > \beta > \frac{3}{4} \rho$  the additive stresses in range  $r$  become infinitely high, notwithstanding the infinitely little work of deformation. Only when  $\beta \geq \rho$ , (complied with by equation (32)), that is, when we choose our arbitrary deformation attitude of the width of wrinkles of the same order (or smaller) as range  $r$ , do the additional stresses become finite in this range.

then  $A_{\max}$  equals  $A_{\min}$ , provided we so choose this deformation that within the whole finite range of the metal sheet (excepting the two infinitely small ranges  $r$ ) the width of wrinkles  $b$  is infinitely small as  $\alpha_E^3$ , and the disturbing range  $r$  at the edge is infinitely small as  $\alpha_E^0$ :

$$\kappa > \beta \geq \frac{3}{4} \rho > 0 \quad (32a)$$

Translation by J. Vanier,  
National Advisory Committee  
for Aeronautics.

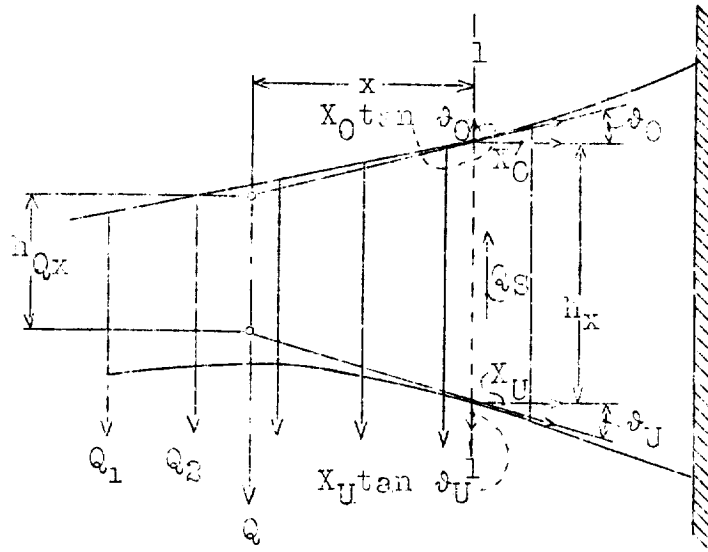


Fig. 14

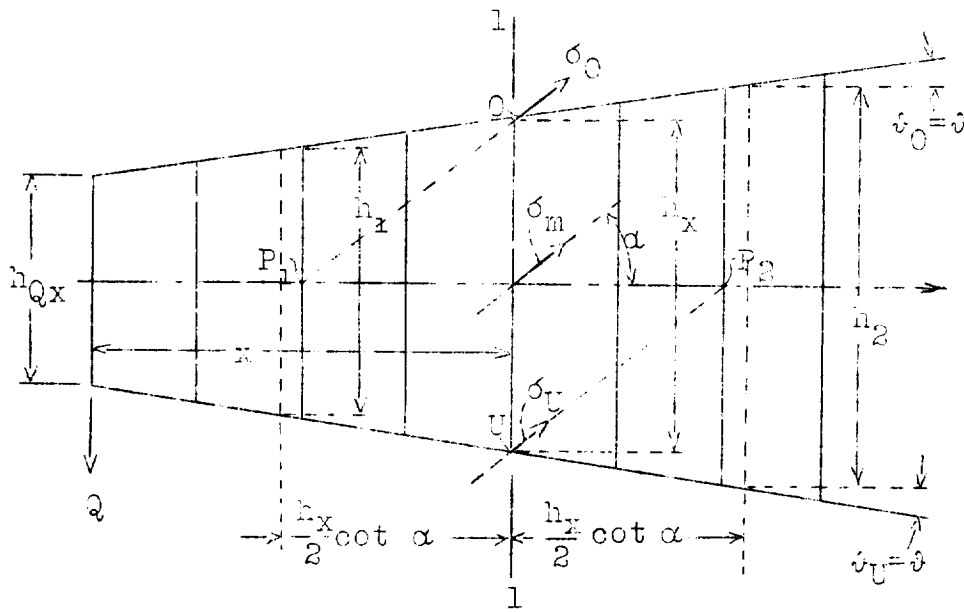


Fig. 15



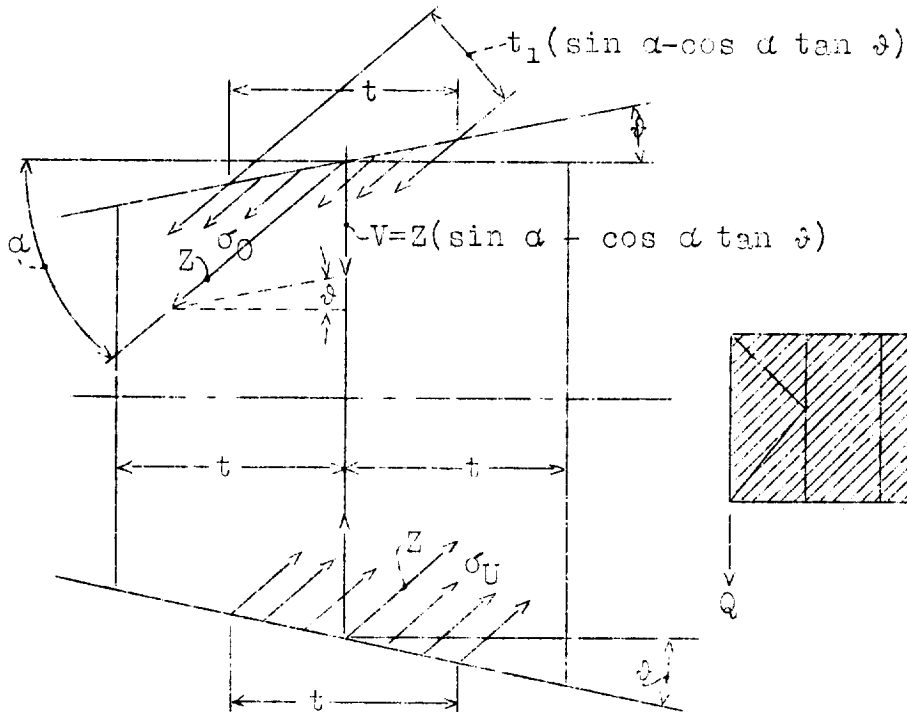


Fig. 16

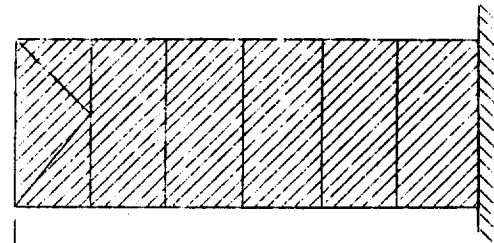


Fig. 17

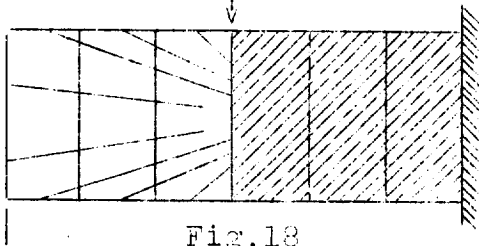


Fig. 18

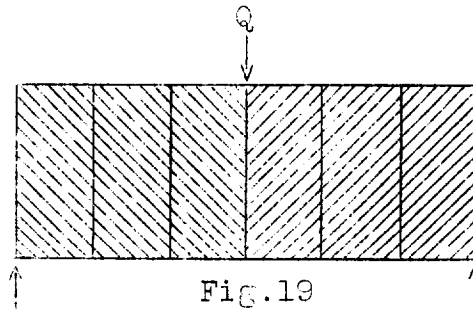


Fig. 19

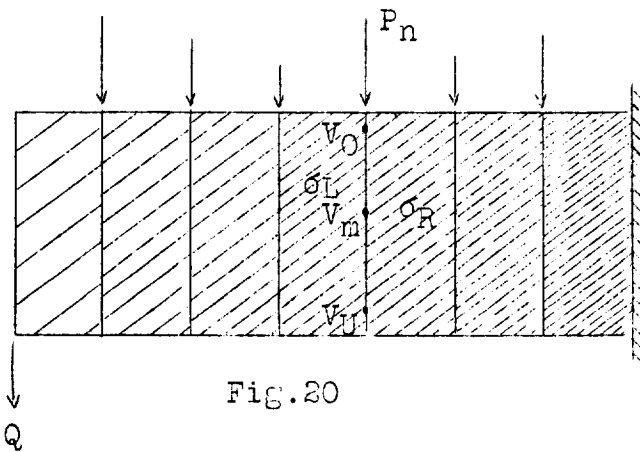


Fig. 20

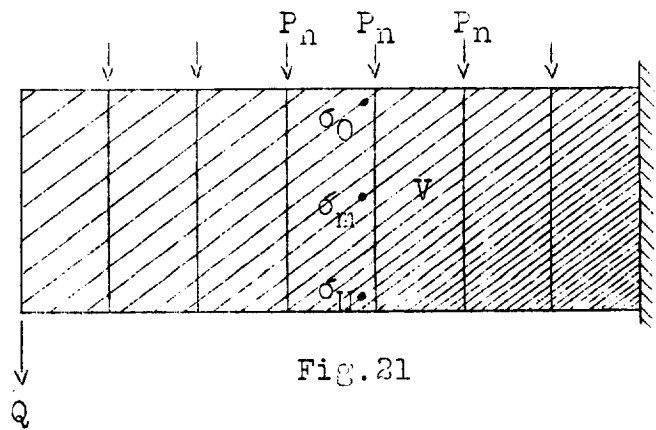


Fig. 21

1. The first part of the document discusses the importance of maintaining accurate records of all transactions and activities. It emphasizes that this is crucial for ensuring transparency and accountability in the organization's operations.

2. The second part of the document outlines the various methods and tools used to collect and analyze data. It highlights the need for consistent and reliable data collection processes to support informed decision-making.

3. The third part of the document focuses on the role of technology in data management and analysis. It discusses how modern software solutions can streamline data collection, storage, and reporting, thereby improving efficiency and accuracy.

4. The fourth part of the document addresses the challenges associated with data management, such as data quality, security, and privacy. It provides strategies to mitigate these risks and ensure that data is used responsibly and ethically.

5. The fifth part of the document concludes by summarizing the key findings and recommendations. It stresses the importance of ongoing monitoring and evaluation to ensure that data management practices remain effective and aligned with the organization's goals.

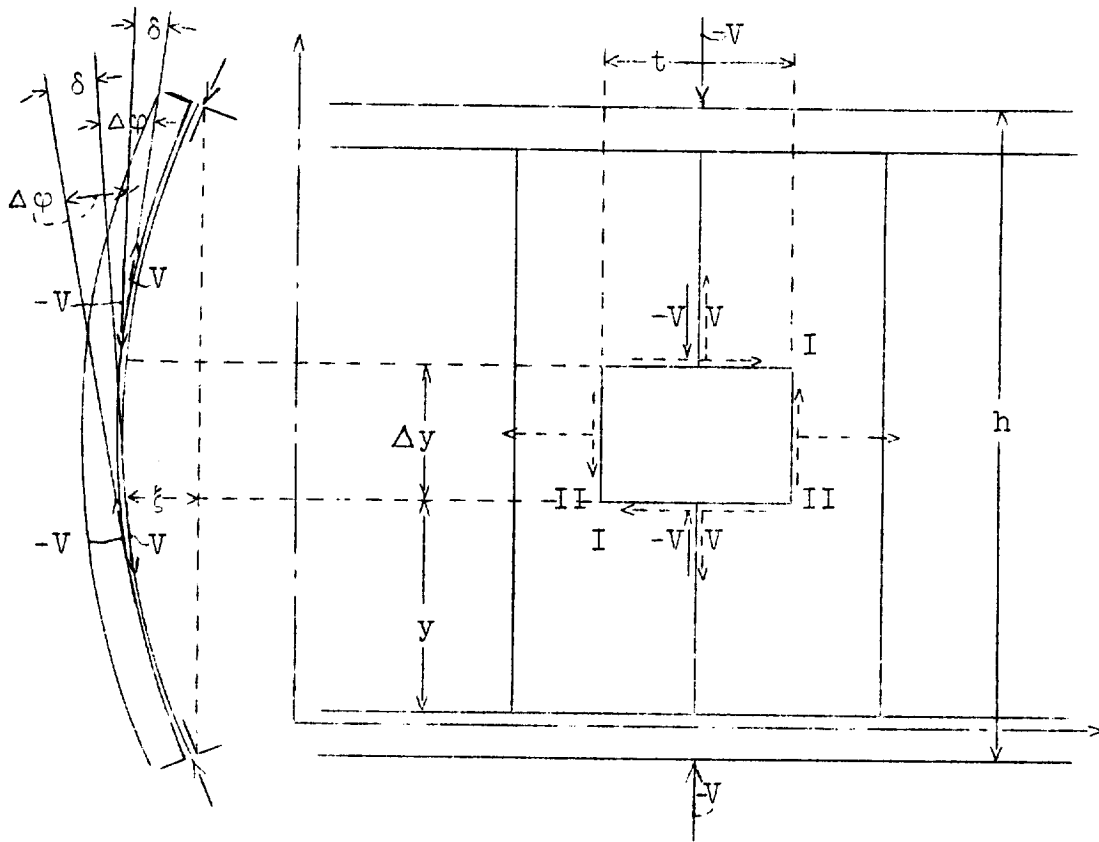


Fig.22

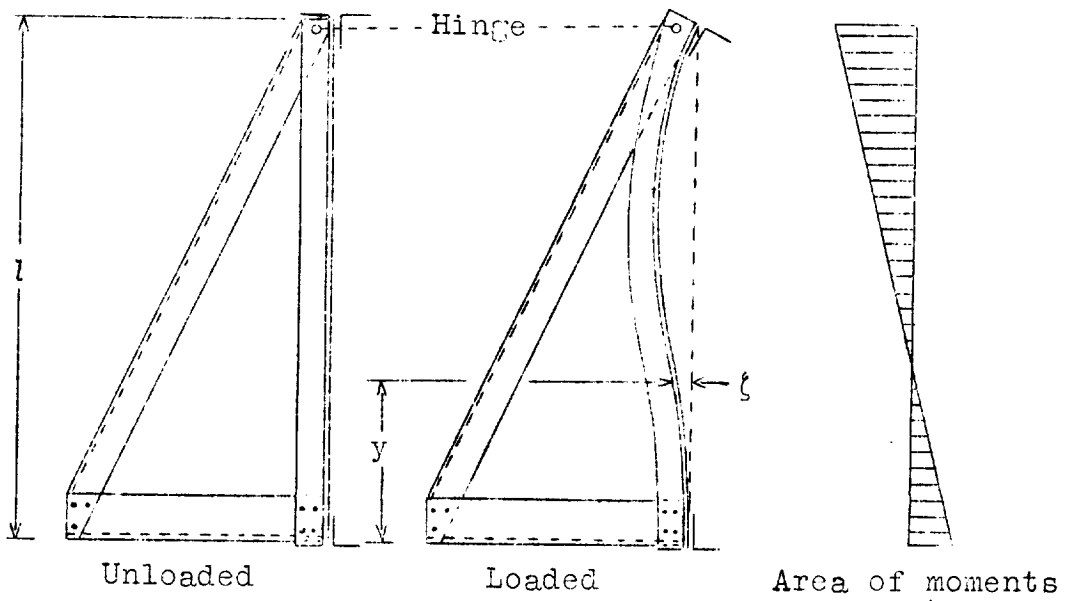


Fig.23



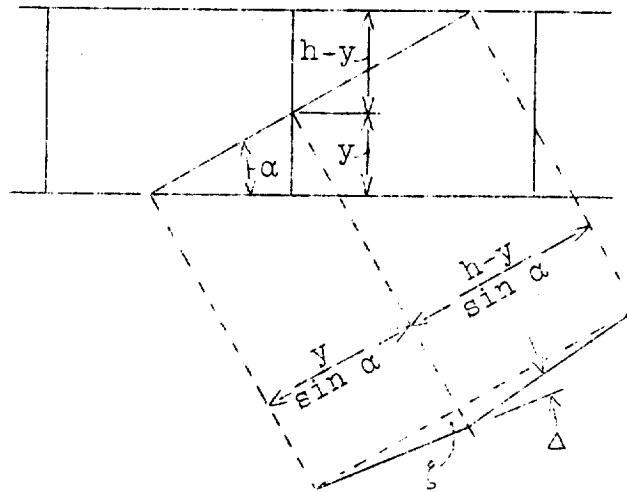


Fig. 24

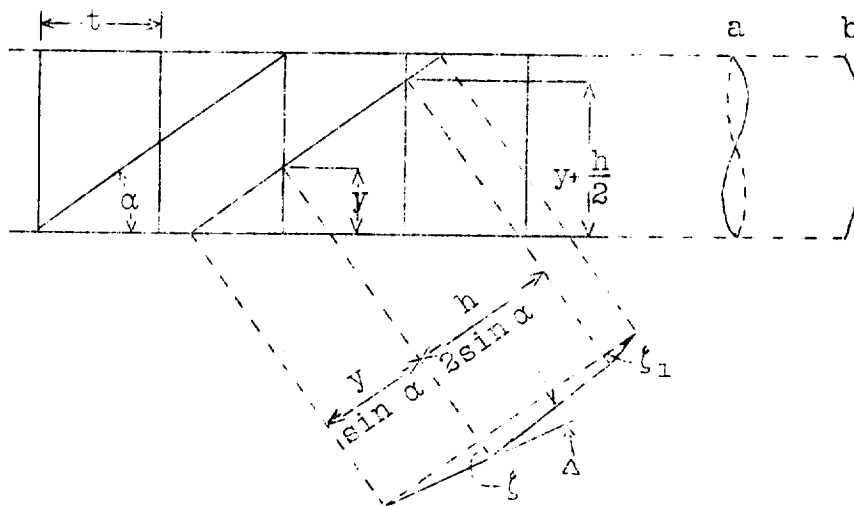


Fig. 25

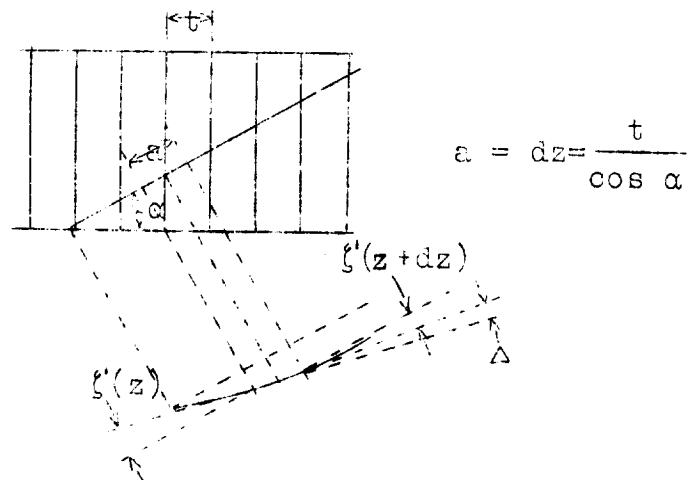
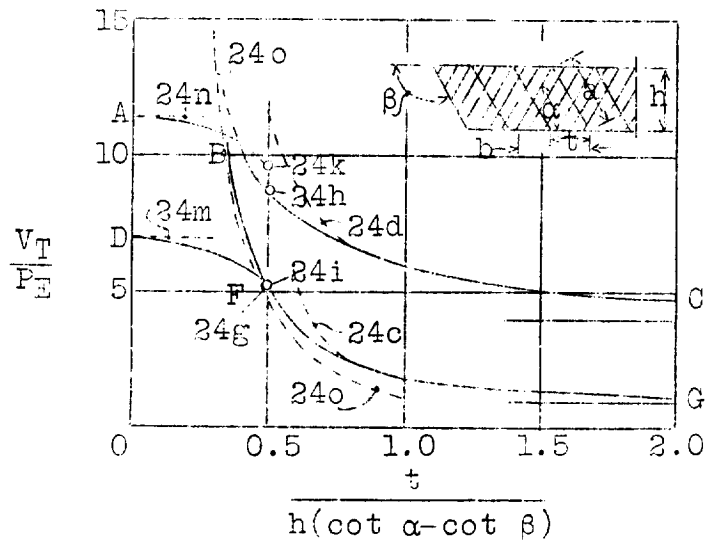


Fig. 26





$$a = h / \sin \beta$$

$$b = h(\cot \alpha - \cot \beta)$$

$$P_E = \pi^2 \frac{EJ}{(h/\sin \beta)^2}$$

Fig. 27

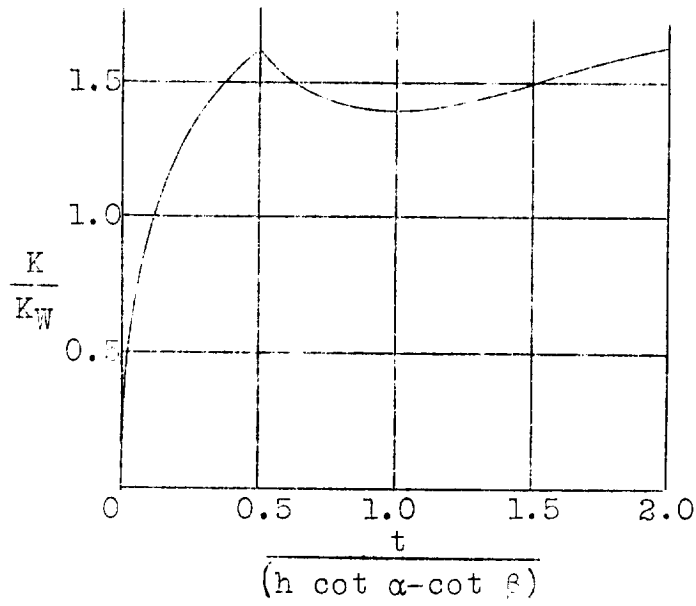


Fig. 28

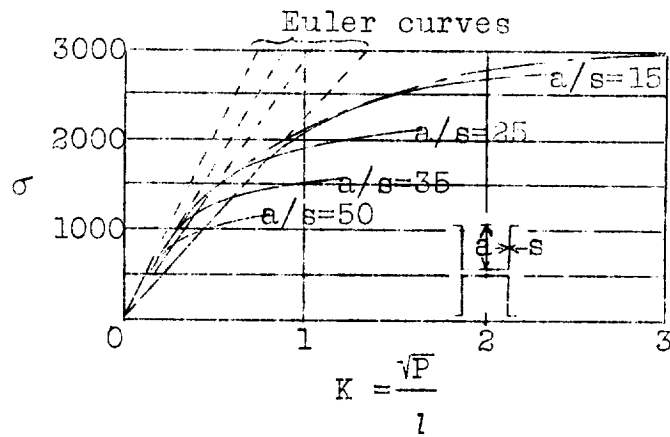


Fig. 29

1. The first part of the document discusses the importance of maintaining accurate records of all transactions and activities. It emphasizes that this is crucial for ensuring transparency and accountability in the organization's operations.

2. The second part of the document outlines the various methods and tools used to collect and analyze data. It highlights the need for a systematic approach to data collection and the importance of using reliable sources of information.

3. The third part of the document focuses on the analysis of the collected data. It discusses the various techniques used to identify trends, patterns, and anomalies in the data, and how these insights can be used to inform decision-making.

4. The fourth part of the document discusses the importance of communication and reporting. It emphasizes that the results of the data analysis should be clearly and concisely communicated to the relevant stakeholders, and that regular reports should be provided to keep them informed of the organization's performance.

5. The fifth part of the document discusses the importance of continuous improvement. It emphasizes that the organization should regularly review its processes and procedures to identify areas for improvement and implement changes to enhance its performance.

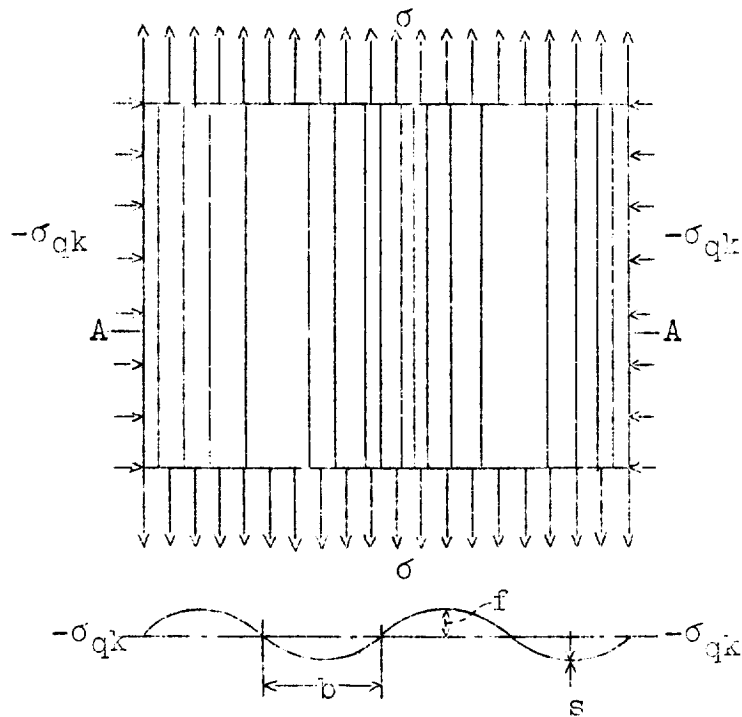


Fig.30

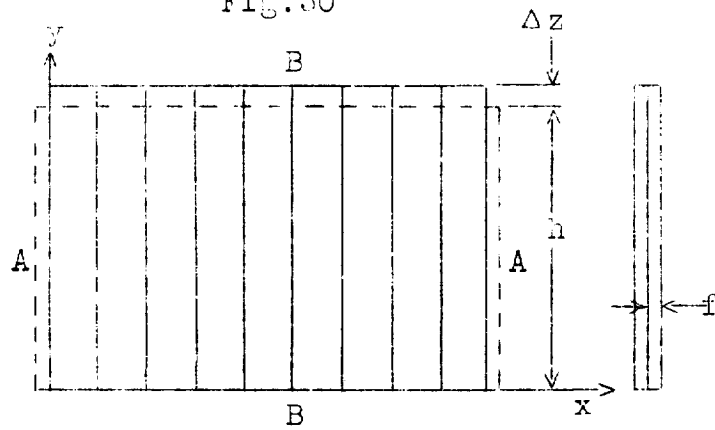


Fig.31

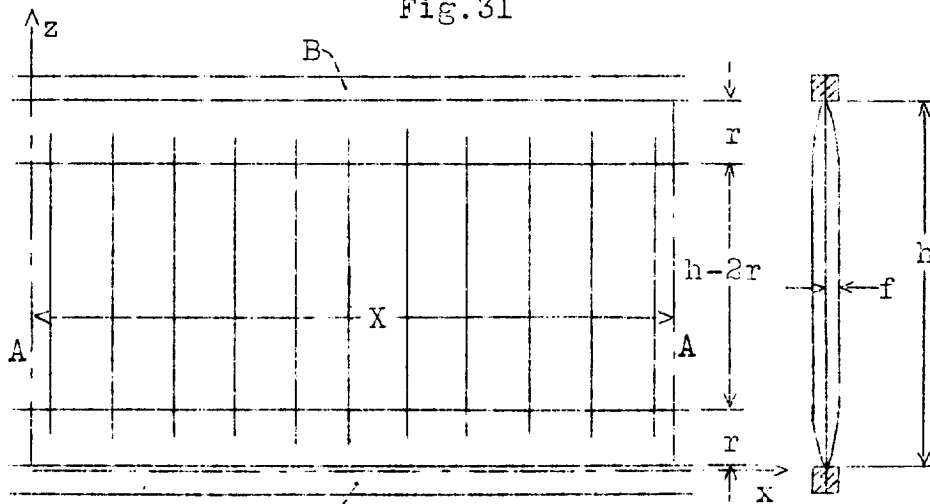


Fig.32

